DocuSign Envelope ID: 2C0AE915-F5FC-4C21-ACD2-CF1A7BDE232A

Efficient use of coolants in heat exchangers for hydrogen tank filling

IFE/E-2023/008

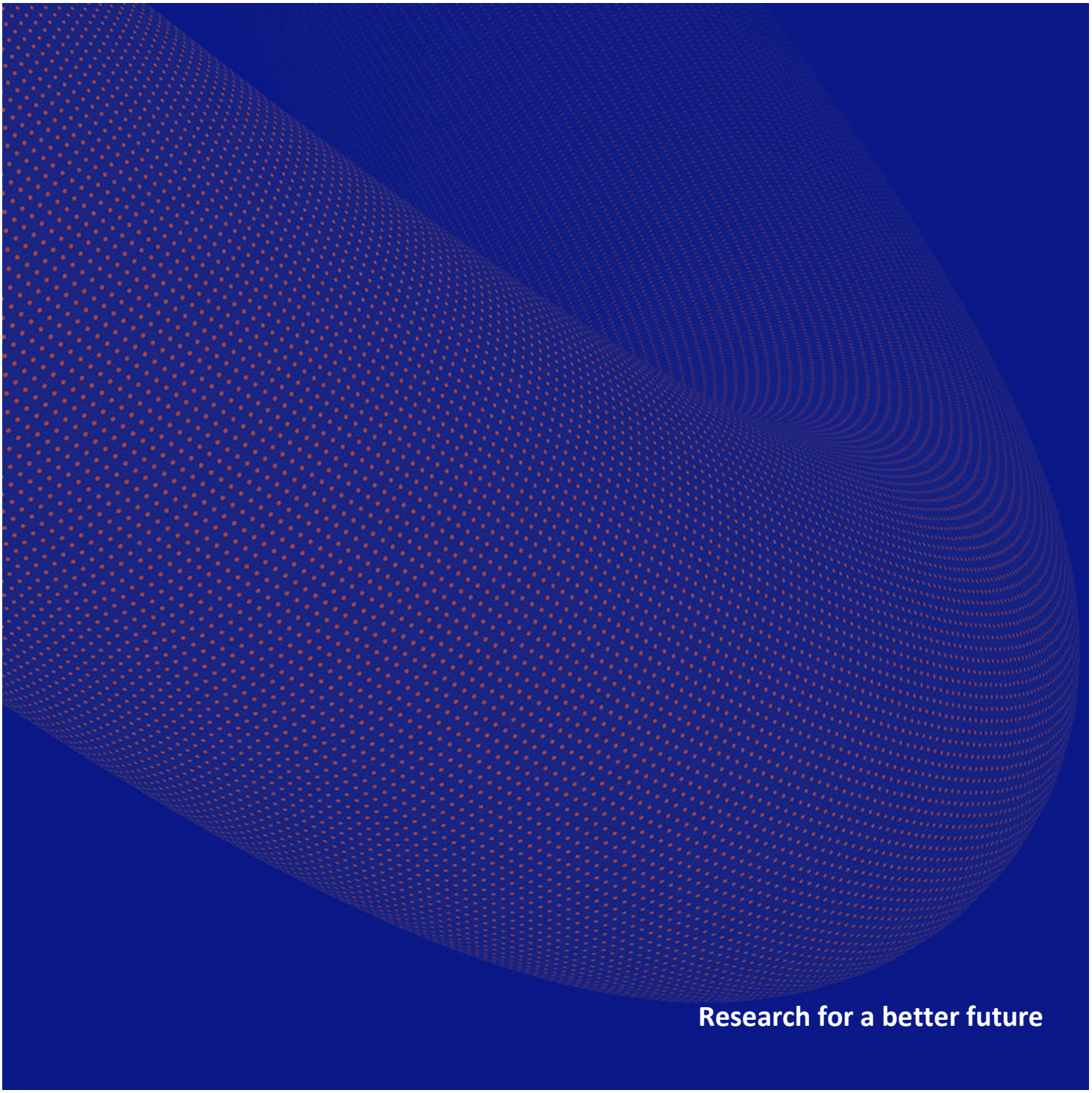

DocuSign Envelope ID: 2C0AE915-F5FC-4C21-ACD2-CF1A7BDE232A

Report number: **IFE/E-2023**/008	ISSN: 2535-6380	Availability: Public	Publication date: 12.10.2023
Revision:	ISBN: 978-82-7017-949-7	DOCUS-ID: 58241	Number of pages: 23

Client:

Title:
Efficient use of coolants in heat exchangers for hydrogen tank filling

Summary:

The purpose of this report is to give some basic facts about heat exchangers and to summarize a series of fluid heat transfer simulations done on a simple counter-flow concentric tube heat exchangers that can be used for hydrogen gas filling systems. The gas and coolant mass flow-rates as well as pressure and temperatures were chosen to be in a range suitable for filling medium sized fuel tanks at hydrogen flow-rates of 1 - 15 kg/min. The possibilities when using some typical coolants, such as water and ethylene glycol-water mixtures, are presented. Effects that limit the efficient heat transfer between hydrogen gas and coolant will be discussed. The appendices give some tables for typical values of heat transfer coefficients as well as the minimum cooling power and the flow-rate needed to fill a hydrogen fuel tank of medium size in a fast and safe way.

Prepared by: 12 October 2023 | 14:09:10 CEST	Geir Helgesen DocuSigned by: Geir Helgesen 4D3ECF7FFB2C42B... External:
Reviewed by: 12 October 2023 | 15:07:16 CEST	Øystein Ulleberg DocuSigned by: 0100F9BD237F4AF...
Approved by: 18 October 2023 | 08:20:02 CEST	Ragnhild Hanche DocuSigned by: Ragnhild Hanche A0DE7A050B5C4EA...
Report distribution:	

Institute for Energy Technology
P.O. Box 40, NO-2027 Kjeller, Norway / P.O. Box 173, NO-1751 Halden
Telephone: +47 63 80 60 00/ +47 69 21 22 00
www.ife.no / firmapost@ife.no

DocuSign Envelope ID: 2C0AE915-F5FC-4C21-ACD2-CF1A7BDE232A

Report
Efficient use of coolants in heat exchangers for hydrogen tank filling

Geir Helgesen

October 12, 2023

Institute for Energy Technology
Department for hydrogen technology
NO-2027 Kjeller, Norway

DocuSign Envelope ID: 2C0AE915-F5FC-4C21-ACD2-CF1A7BDE232A

Contents

1 Introduction **5**

2 Heat exchangers **5**

2.1 Some theory of counter-flow heat exchanger systems 6

3 Computational fluid dynamics simulations of heat exchanger **7**

3.1 The model system computation 8

3.2 Choosing the right coolant 8

3.3 Influence of gas pressure on cooling capacity 12

3.4 Thermal behavour of coolants in heat exchangers 12

3.5 Flow patterns in the heat exchanger 14

4 Discussion **16**

A Appendix 1: Dimensionless numbers in heat exchangers **20**

B Appendix 2: Heat transfer coefficients **21**

C Appendix 3: Cooling capacity **22**

DocuSign Envelope ID: 2C0AE915-F5FC-4C21-ACD2-CF1A7BDE232A

List of symbols

.

A_s..... surface area of heat exchanger
c_p..... specific heat capacity (unit J/kg·K)
C_r..... capacity ratio
$\dot{C}_h$, $\dot{C}_c$..... hot and cold heat flow capacities ($= \dot{m}c_p$, unit W/K)
H..... enthalpy
h_i, h_o..... heat convection coefficient of inner and outer fluid (unit W/K·m)
k..... thermal conductivity of tube metal wall (unit W/K·m)
L..... tube length
$\mathcal{L}$..... typical/characteristic length scale
LMTD, ΔT_{lm}..... log-mean temperature difference (unit K)
$\dot{m}_h$, $\dot{m}_{H2}$..... mass flow-rate of hot fluid or hydrogen gas (unit kg/s)
$\dot{m}_c$, $\dot{m}_{H2O}$..... mass flow-rate of cold fluid, coolant or water (unit kg/s)
NTU..... number of transfer units
P_{in}, P_{out}..... inlet and outlet gas pressures
Pr..... Prandtl number
$\dot{Q}$..... cooling power, heat transfer rate (unit kW)
R..... thermal resistance (unit K/W)
r_i, r_o..... inner and outer tube radius
Re..... Reynolds number
$T_{h,in}$, $T_{h,out}$, $T_{c,in}$, $T_{c,out}$..... inlet and outlet temperatures of hot and cold fluids
U..... effective heat transfer coefficient (unit $\mathrm{W/m^2 \cdot K}$)
v, v_g, v_{cool}..... velocity of gas and coolant (unit m/s)
ΔT..... temperature drop in hydrogen gas
ε..... effectiveness of heat exchanger
η..... dynamic viscosity of fluid (unit Pa·s)
ρ..... density of fluid (unit $\mathrm{kg/m^3}$)

DocuSign Envelope ID: 2C0AE915-F5FC-4C21-ACD2-CF1A7BDE232A

Abstract

The purpose of this report is to give some basic facts about heat exchangers and to summarize a series of fluid heat transfer simulations done on a simple counter-flow concentric tube heat exchangers that can be used for hydrogen gas filling systems. The gas and coolant mass flow-rates as well as pressure and temperatures were chosen to be in a range suitable for filling medium sized fuel tanks at hydrogen flow-rates of 1 - 15 kg/min. The possibilities when using some typical coolants, such as water and ethylene glycol-water mixtures, are presented. Effects that limit the efficient heat transfer between hydrogen gas and coolant will be discussed. The appendices give some tables for typical values of heat transfer coefficients as well as the minimum cooling power and the flow-rate needed to fill a hydrogen fuel tank of medium size in a fast and safe way.

DocuSign Envelope ID: 2C0AE915-F5FC-4C21-ACD2-CF1A7BDE232A

1 Introduction

The use of hydrogen as an energy carrier is moving into new sectors of the society and in particular into the transportation sector. Car, buses, and trucks are now running on hydrogen gas (H_2). In the marine shipping sector, compressed hydrogen gas and even liquid hydrogen are slowly being introduced as fuel source for propulsion of cargo ships and ferries. Even in aviation, hydrogen is being tested. Finally, hydrogen is now being explored for use in trains and locomotives. The European Rail4EARTH-project, which is funded by the Europe's Rail Joint Undertaking [1], explores the different aspects of replacing diesel as fuel on rail tracks that cannot be supplied by power from electrified lines. Important aspects to be studied are fuel cells for use on the rolling stock, the train hydrogen refueling stations, and the safety aspects of using hydrogen. Since battery powered trains are limited to about 150 km autonomous operation on batteries (goal in Rail4EARTH is to extend range to 200 km), hydrogen solution with fuel cells will be needed for longer distances, up to 1000 km between refueling. Passenger trains with 150-200 seats and 2-3 cargoes will typically need four onboard storage tanks containing about 100 kg of H_2 at 350 bar pressure. The fueling time at the station should not be more than about 15 min. These trains can run at speeds up to 160 km/h and may need a max power up to 1.7 MW. At the fueling station, the compressed gas can be produced locally by electrolyzing units with capacity of about 200 kg of H_2 per day and will be stored in fixed or mobile units with capacity of up to about 200 kg H_2 at 500 bar. In order to reduce heating of the H_2 during filling, heat exchanger cooling systems have to be installed at the filling station. Different from most other gases, H_2 has a negative Joule-Thomson coefficient, $\left(\frac{\partial P}{\partial T}\right)_H \approx -0.03$ K/bar, near room temperature. This means that the gas will heat up during filling into a nearly empty tank, and pre-cooling in a heat exchanger may be needed to avoid heating above the upper temperature limit of the tank.

2 Heat exchangers

Heat exchangers (HX) come in a variety of different types [2, 3, 4, 5]. The simplest are double pipe heat exchangers where one fluid is flowing in a tube mounted inside an outer tube containing another fluid (liquid or gas) - the coolant - in its "annulus region". These systems come in two main types, *parallel flow* with both fluids entering on the same side and *counter flow* where the flow direction of the fluids are opposite (see Fig. 1). Such double pipe exchangers can also be made into more complex, bent shapes (e.g. *multi-pass HX*), and fins can be added to increase the effective surfaces area between the two fluids.

In other types of heat exchangers, the flow directions of the fluids are perpendicular to each other, so-called *cross-flow HX*. Also, larger shell-and-tube heat exchangers, which have a large number of tubes packed into an outer shell, are used in industrial applications. Larger temperature changes in one of the fluids can be obtained by using condensers or evaporators. In these, one of the fluids transfer or absorb heat from the other fluid by changing from gas to liquid state (or the opposite).

The capacity of a heat exchanger will depend on its field of application. For bunkering of ships and ferries, several tons of hydrogen need to be transferred in one hour or less, which implies a mass transfer rate of 0.5 kg/s or more. For cars a typical tank of 100 l can contain 6 kg at 700 bar and will be filled in less than 5 min, corresponding to a mass transfer rate

DocuSign Envelope ID: 2C0AE915-F5FC-4C21-ACD2-CF1A7BDE232A

of 0.02 kg/s. Filling 100 kg to a train in 15 min, gives a transfer rate of 0.1 kg/s. Thus, the construction, capacity and capability of the heat exchanger will differ in these cases, heavily dependent on the gas transfer rate. These differences will be explored in the following sections.

2.1 Some theory of counter-flow heat exchanger systems

In double pipe heat exchangers the thermal resistance R to heat transfer from hot fluid to the colder fluid can be modeled similar to a resistor network

$$R_{total} = R_{inner} + R_{wall} + R_{outer} = \frac{1}{h_i 2\pi r_i} + \frac{\ln\left(r_o/r_i\right)}{2\pi k L} + \frac{1}{h_o 2\pi r_o} = \frac{1}{U \cdot A_s}, \tag{1}$$

where h_i, h_o, and k are the *heat convection coefficients* of the inner and outer fluid, and the thermal conductivity of the tube metal, respectively, while r_i and r_o are radius of the inner and outer concentric tubes, and L is the length of the tubes. U is called the *effective heat transfer coefficient* and A_s is the effective heat transfer surface. The effective heat transfer coefficient in units of $\mathrm{W/m^2 \cdot K}$ vary from 10-40 for gas-to-gas systems to 1000 or more for liquid-liquid systems (e.g. water-to-water) and can reach up to 10000 for evaporators and condensers. The product $U \cdot A_s$ (in $\mathrm{W/K}$) is the important parameter for characterizing a heat exchanger system. It is the transferred heat per degree of temperature difference between the fluids.

The heat transfer will be dominated by the smallest heat transfer coefficient of the fluids if they are significantly different. In many cases the thermal resistance in the wall R_{wall} can be neglected (i.e. thin wall) and if $h_1 \ll h_2$ (1 or 2 being inner or outer fluid), then $U \sim h_1$. This can often occur when one fluid is a gas and the other is a liquid.

In order to characterize heat exchangers, various characteristic numbers are used. To have *one* typical number for the temperature difference between the two sides, the *Log-Mean Temperature Difference* (LMTD) is often used. LMTD can be defined as

$$\Delta T_{lm} = \frac{\Delta T_1 - \Delta T_2}{\ln\left(\Delta T_1/\Delta T 2_1\right)}, \tag{2}$$

and the *effective heat transfer rate* $\dot{Q}$ can be calculated as

$$\dot{Q} = U A_s \Delta T_{lm}. \tag{3}$$

The definitions of the temperature differences ΔT_1 and ΔT_2 depend on the type of double pipe HX. Using subscripts h and c for hot and cold flow, then for counter-flow $\Delta T_1 = T_{h,in} - T_{c,out}$

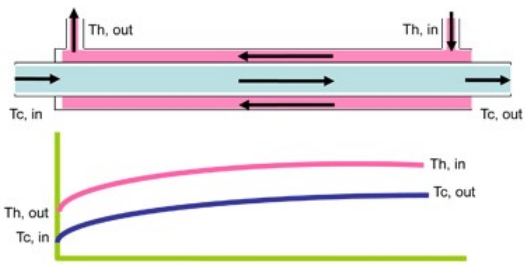

Figure 1: Counter-flow heat exchanger (top) and temperature variations within the hot and cold flows. (Adapted from [6].)

DocuSign Envelope ID: 2C0AE915-F5FC-4C21-ACD2-CF1A7BDE232A

and $\Delta T_2 = T_{h,out} - T_{c,in}$, i.e., the temperature differences at the hot-in side and hot-out side, respectively. [1] It can be shown that LMTD for for a counter-flow heat exchanger will always be larger than that for a similar parallel flow HX, and thus will be more energy efficient. For more complex types of heat exchangers, a correction factor for the shape has to be taken into the definition of LMTD.

With $\dot{m}_c$ and $\dot{m}_h$ being the mass flow-rate (in kg/s) of the cold and hot fluids and c_p being their heat capacities, one can define the heat flow capacities $\dot{C}_h = \dot{m}_h c_{p,h}$ and $\dot{C}_c = \dot{m}_c c_{p,c}$ of the hot and cold fluids.

The effectiveness ε of a heat exchanger depends on its geometry and on the flow arrangement. Now, assuming $\dot{C}_c > \dot{C}_h$, the effectiveness is defined as

$$\varepsilon = \frac{\dot{Q}}{\dot{Q}_{max}} = \frac{T_{h,in} - T_{h,out}}{T_{h,in} - T_{c,in}}. \tag{4}$$

If $\dot{C}_c < \dot{C}_h$, then $T_{h,in} - T_{h,out}$ is replaced by $T_{c,out,} - T_{c,in}$ in the equation above.

Thus, the overall heat transfer coefficient U is the most important parameter for a given HX system, and when this and the contact surface A_s are known, the hot and cold outlet temperatures can be calculated. With $\dot{C}_{min}$ and $\dot{C}_{max}$ being the smallest and largest, respectively, of $\dot{C}_c$ and $\dot{C}_h$, the maximum possible value of heat transfer between the two fluids will be $\dot{Q}_{max} = \dot{C}_{min}\left(T_{h,in} - T_{c,in}\right)$. Now, defining $\frac{1}{\dot{C}_{diff}} = \frac{1}{\dot{C}_{min}} - \frac{1}{\dot{C}_{max}}$, it can be shown that

$$\varepsilon = \frac{1 - \exp\left(-\frac{UA_s}{\dot{C}_{diff}}\right)}{1 - \frac{\dot{C}_{min}}{\dot{C}_{max}} \cdot \exp\left(-\frac{UA_s}{\dot{C}_{diff}}\right)}. \tag{5}$$

The outlet temperatures are then:

$$T_{h,out} = T_{h,in} - \varepsilon\left(T_{h,in} - T_{c,in}\right) \tag{6}$$

$$T_{c,out} = T_{c,in} + \frac{\dot{C}_{min}}{\dot{C}_{max}}\left(T_{h,in} - T_{h,out}\right) \tag{7}$$

The heat transfer in heat exchangers can be generalized by introducing dimensionless numbers, such as capacity ratio C_r, effectiveness ε, and NTU, as described in Appendix 1.

3 Computational fluid dynamics simulations of heat exchanger

Heat transfer rate $\dot{Q}$ and effectiveness ε for heat exchangers can be estimated based on tabulated values. However, in order to get a realistic and detailed information on how a heat exchanger will perform during hydrogen tank filling, detailed computer simulations based on the laws of thermodynamics and fluid flow are needed. Using finite element computer simulations tools such as the commercial software package COMSOL Multiphysics [7], specific values of $U \cdot A_s$ can be obtained under relevant and realistic gas filling conditions.

In the current study, a model of a horizontal and straight, 10 m long, concentric counter-flow heat exchanger was used to calculate values of the temperature drop $\Delta T = T_{H2,in} - T_{H2,out}$ in the H_2 gas and heat transfer rate $\dot{Q}$ when the temperatures and mass flow rates

[1] For parallel flow HX $\Delta T_1 = T_{h,in} - T_{c,in}$ and $\Delta T_2 = T_{h,out} - T_{c,out}$.

DocuSign Envelope ID: 2C0AE915-F5FC-4C21-ACD2-CF1A7BDE232A

of gas and coolant were input parameters in the simulations. Pure water and mixtures of ethylene glycol and water were used as coolants.

In general, the values of the heat transfer coefficient U is smaller for EG-water mixtures than for pure water. However, a lower temperature $T_{c,in}$ of the coolant may compensate for a smaller value of U and give a better overall cooling effect in the end.[8] According to the international SAE-protocol for filling of heavy duty vehicles [9], the temperature of *type-4* composite material hydrogen gas tanks needs to be kept below 85 °C (358 K) in order to avoid thermal damage to the inner polymer lining of the tanks. For railroad and other large scale users of compressed H_2, there exists so far no international filling protocol. However, one may assume that a similar temperature limit will apply for high transfer-rate filling of larger tanks composed of similar materials.

3.1 The model system computation

The model was constructed using the COMSOL Multiphysics 5.6 software, including the heat transfer and microfluidics modules. The basic model consisted of an inner tube of radius $r_i =$ 10 mm and wall thickness $t = 1$ mm and length L =10 m. The outer concentric tube for the coolant had a radius of r_o =15 mm with same wall thickness and length. The tube material used in the simulations was structural steel, and heat exchange from the outer tube to the HX surroundings at ambient temperature was neglected. This is a good approximation if the temperate of the coolant is not very low, as when using water cooling, and for coolants having lower temperature when using thermal insulation of the heat exchanger. The exit pressure of the coolant was assumed to be ambient pressure at 1 bar, and the exit pressure P_{out} of the hydrogen gas on leaving the HX could be varied in the relevant range for filling typical compressed gas tanks, 20 bar $< P_{out} <$ 450 bar. From the HX tube dimensions and the mass flow-rates $\dot{m}_{H2}$ of gas and $\dot{m}_c$ of coolant, the pressure drop for gas and coolant was calculated in the simulations. Since the Reynolds numbers for the flow of both phases can be quite high, an "algebraic yplus" turbulent flow mode of COMSOL was used for both, and no-slip boundary condition was applied. The layered material option in COMSOL was used for handling the thin wall between the fluids, and the mesh was adjusted to get reliable precision in the relevant flow regime.

3.2 Choosing the right coolant

In addition to water, various other fluids may be used as coolants in heat exchanger systems. Due to low toxicity and good performance, mixtures of ethylene glycol and water are commonly used for cooling in the temperature range from 0 °C down to −41 °C (232 K). In this study water mixtures containing 20-60 % ethylene glycol (EG) have been explored in addition to pure water as coolant. Since the flow in the gas will be turbulent for all mass flow rates, the thermal conductivity plays a minor role. This also applies for the coolant under most flow conditions. It is then only their heat capacity and the viscosity, which determine the Reynolds number, that are important parameters. Figure 2 shows how the viscosity and the heat capacity of the relevant mixtures, as well as those of water, vary with temperature.

A series of simulations were done to calculate the heat exchange coefficient U and the temperature drop ΔT_{H2} for the gas after passing the heat exchanger. The temperature of

DocuSign Envelope ID: 2C0AE915-F5FC-4C21-ACD2-CF1A7BDE232A

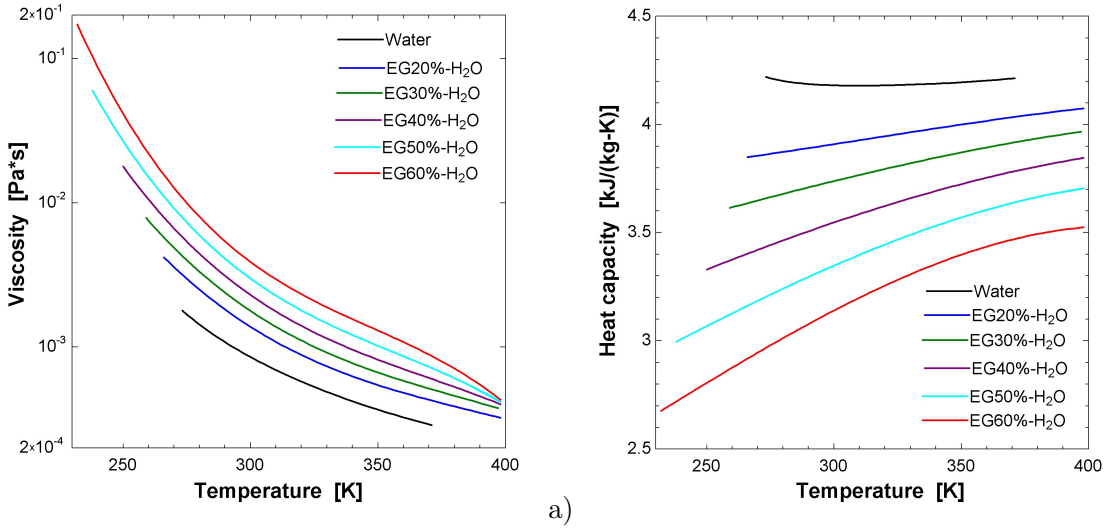

Figure 2: a) Viscosity of water and various ethylene glycol-water mixtures. Note the logarithmic y-axis. b) Heat capacity of EG-water mixtures.

the hydrogen at the inlet was assumed to be $T_{H2,in} = 25\,°\mathrm{C} = 298\,\mathrm{K}$, and in most cases the exit pressure from the HX was set to $P_{out} = 100$ bar, which corresponds to typical pressure during tank filling. The gas mass flow-rates were in the range 0.01 kg/s $\leq \dot{m}_{H2} \leq$ 0.2 kg/s (or 0.6 kg/min $\leq \dot{m}_{H2} \leq$ 12 kg/min), which may be relevant flow-rates for filling of medium-sized hydrogen tanks like those for trains and smaller boats. The coolant flow-rates were chosen to be in the range 0.05 kg/s $\leq \dot{m}_c \leq$ 1.0 kg/s. The lowest allowable temperature T_c for the coolant was chosen in each case, ranging from T_c= 274 K for water and T_c= 266 K for the 20% EG-water mixture, down to T_c= 232 K for an EG concentration of 60 %. Examples of results from the smallest and largest gas flow-rates, $\dot{m}_{H2} = 0.01$ kg/s and $\dot{m}_{H2} = 0.2$ kg/s respectively, are shown in Figs. 3 and 4, respectively. These figures show that the overall heat exchange coefficient U drops with increasing concentration of ethylene glycol. However, this drop in the values of U was fully or partly compensated for by the lower coolant inlet temperature $T_{c,in}$ that could be used as the concentration of EG was increased. As Fig. 3b) shows, for small flow-rates of H_2, here $\dot{m}_{H2} = 0.01$ kg/s, the gas exit temperature dropped with increased EG concentration as well as with increased coolant flow-rate $\dot{m}_c$. For "medium" gas flow-rates like $\dot{m}_{H2} = 0.2$ kg/s, shown in Fig. 4b), there were no or only minor changes in exit temperature as function of EG concentration as the gas flow-rate increased. The temperature drop with increasing coolant flow-rates was as expected.

In order to explore these effects closer, the same simulation was repeated for pure water coolant and for 30% and 50% EG in water using some typical values of $\dot{m}_{H2}$ and $\dot{m}_c$. The results are shown as 3D bar diagrams in Fig. 5. As seen for water coolant in Fig. 5a), for low H_2 flow-rates like $\dot{m}_{H2} \leq 0.02$ kg/s, the temperature drop reached its maximum $\Delta T \approx$ 21 K near $\dot{m}_c$ = 0.1-0.2 kg/s with hardly any increase for coolant flow-rates beyond that. For higher hydrogen flow-rates $\dot{m}_{H2} \geq$0.05 kg/s, the temperature drop decreased with increasing gas flow-rate and increased with increasing water coolant flow-rate. This is as one would expect. The situation was quite similar for an EG concentration of 30%, which is shown in Fig. 5b). But now the maximum temperature drop was about 36-38 K. For 50% EG in water, the temperature drop increased with $\dot{m}_c$ for all values of $\dot{m}_{H2}$ and decreased with

DocuSign Envelope ID: 2C0AE915-F5FC-4C21-ACD2-CF1A7BDE232A

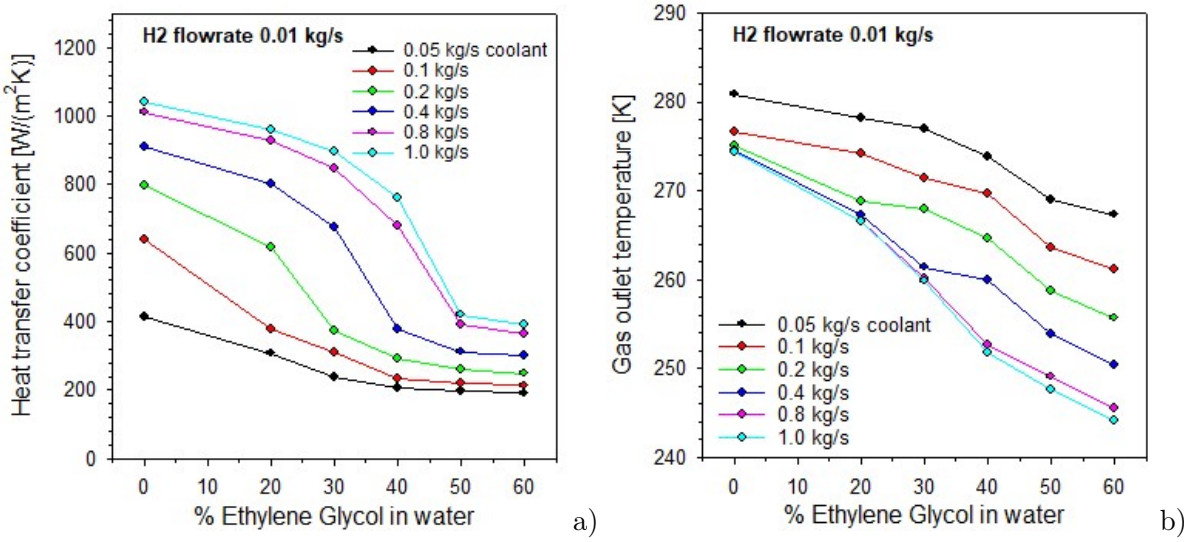

Figure 3: a) Heat transfer coefficient U and b) HX exit temperature T_{out} vs. % of EG in an ethylene glycol-water mixture for **very small mass flow-rate** of H_2 - $\dot{m}_{H2} = 0.01$ kg/s.

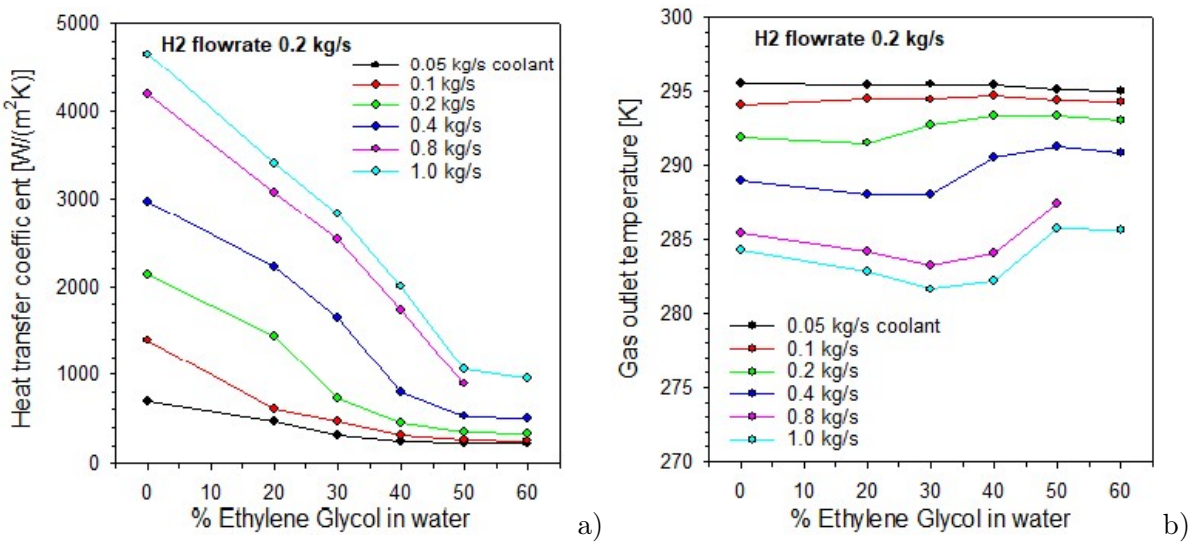

Figure 4: a) Heat transfer coefficient U and b) HX exit temperature T_{out} vs. % of EG in an ethylene glycol-water mixture for **relatively large mass flow-rate** of H_2 - $\dot{m}_{H2} = 0.2$ kg/s. The inlet temperature of gas was $T_{in} = 298$ K.

DocuSign Envelope ID: 2C0AE915-F5FC-4C21-ACD2-CF1A7BDE232A

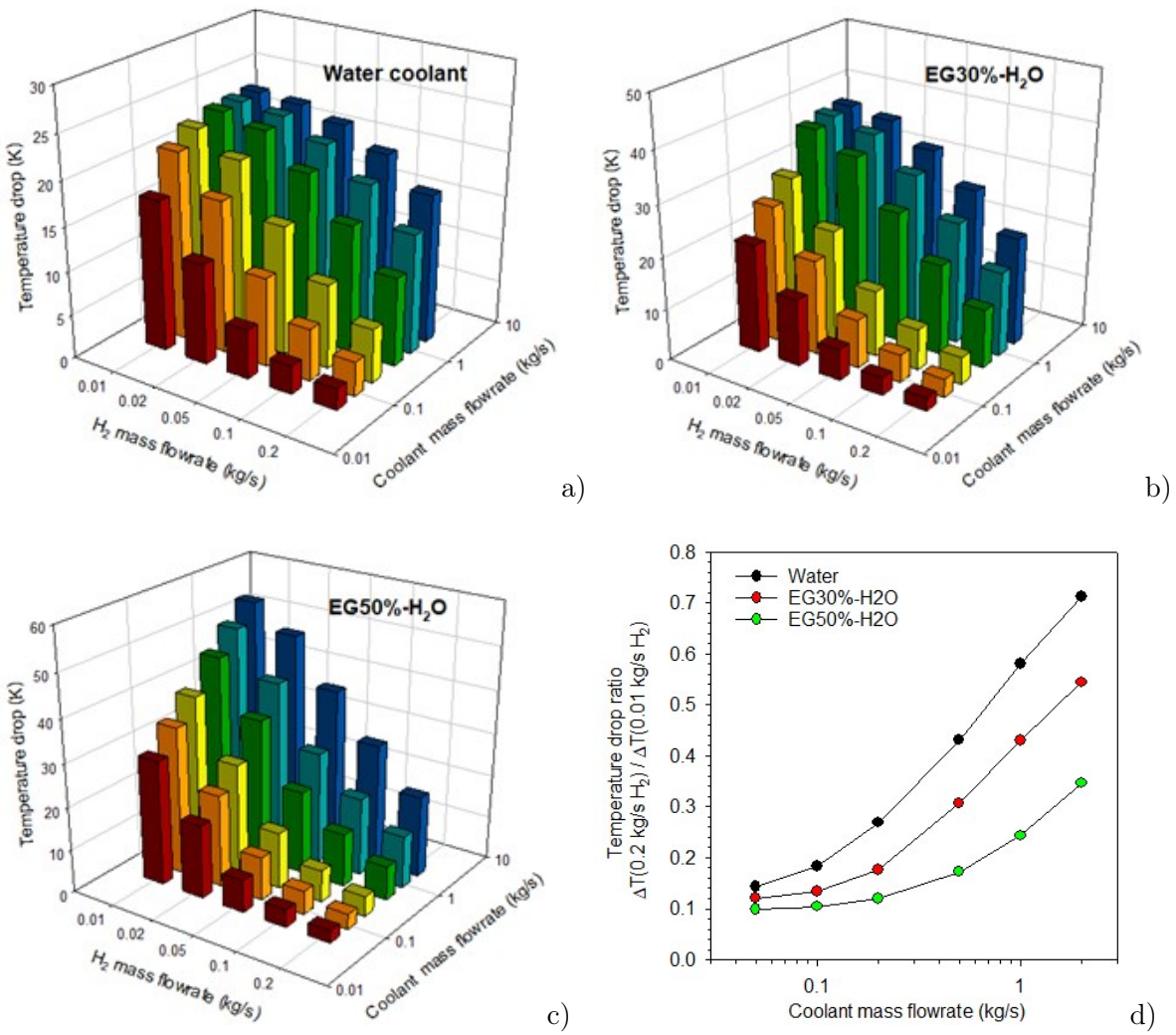

Figure 5: Temperature drop ΔT vs. hydrogen and coolant mass flow-rates for a) water coolant $-$ T_c =274 K, b) EG30%-water $-$ T_c =259 K, and c) EG50%-water $-$ T_c =238 K. The inlet temperature of H_2-gas was 298 K. d) Calculated ratio between ΔT-values of the largest and the smallest gas flow-rate $\Delta T(\dot{m}_{H2} = 0.2\,\mathrm{kg/s})/\Delta T(\dot{m}_{H2} = 0.1\,\mathrm{kg/s})$ as function of coolant flow-rate.

increasing $\dot{m}_{H2}$. The maximum value in this case was $\Delta T = 54.5$ K.

To more clearly see how the cooling effect was affected by flow-rates, one may compare the temperature drop for higher H_2 flow-rates to those for lower flow-rates. Figure. 5d) shows the ratio of ΔT for $\dot{m}_{H2} = 0.2$ kg/s to that for $\dot{m}_{H2} = 0.01$ kg/s, i.e., $\Delta T(0.2\mathrm{kg/s})/\Delta T(0.01\mathrm{kg/s})$ vs. $\dot{m}_c$. For water as coolant this ratio is nearly linear in this plot which has a logarithmic x-axis. The ratio approaches 1 on the y-axis, which indicates a very efficient heat transfer in water for $\dot{m}_c > 2$ kg/s. Thus, the cooling capacity cannot be much improved using higher coolant flow-rates in the $\dot{m}_{H2} = 0.2$ kg/s case. However, for the EG50%-water mixture (green curve in the figure) there still can be much to gain in the cooling for the highest gas flow-rate by a further increase in coolant flow $\dot{m}_c$. The behaviour in this last case can be seen as result of the coolant not having "fully utilized" its maximum cooling capacity. The reason for this is further explored in Section 3.4 below.

DocuSign Envelope ID: 2C0AE915-F5FC-4C21-ACD2-CF1A7BDE232A

3.3 Influence of gas pressure on cooling capacity

Since the density of a gas will depend on the gas pressure, it is interesting to see how heat exchange coefficients and the temperature drop behave at lower pressures, i.e., in the initial phase of filling a tank. A series of calculations were done for the same coolants as above but varying the gas exit pressure P_{out} from 10 bar to 300 bar, and, thus, having an increased H_2 density. The mass flow-rate was kept fixed at the value $\dot{m}_{H2} = 0.1$ kg/s. For all the studied coolants, the heat transfer coefficient U was nearly pressure independent for pressures above $P_{out} = 20$ bar (data not shown here).

The results for the temperature drop ΔT vs. exit pressure for water and EG50%-water are shown in Fig. 6. The resulting values of ΔT were nearly constant above P_{out} =100 bar, but show a strong decrease between 10 bar and about 30 bar pressure for all coolant flow-rates. This effect was strongest for the lowest values of $\dot{m}_c$ and when using water as a coolant as can be seen in Fig. 6a). This is a result of the low density at low pressures, which makes heat transfer easy.

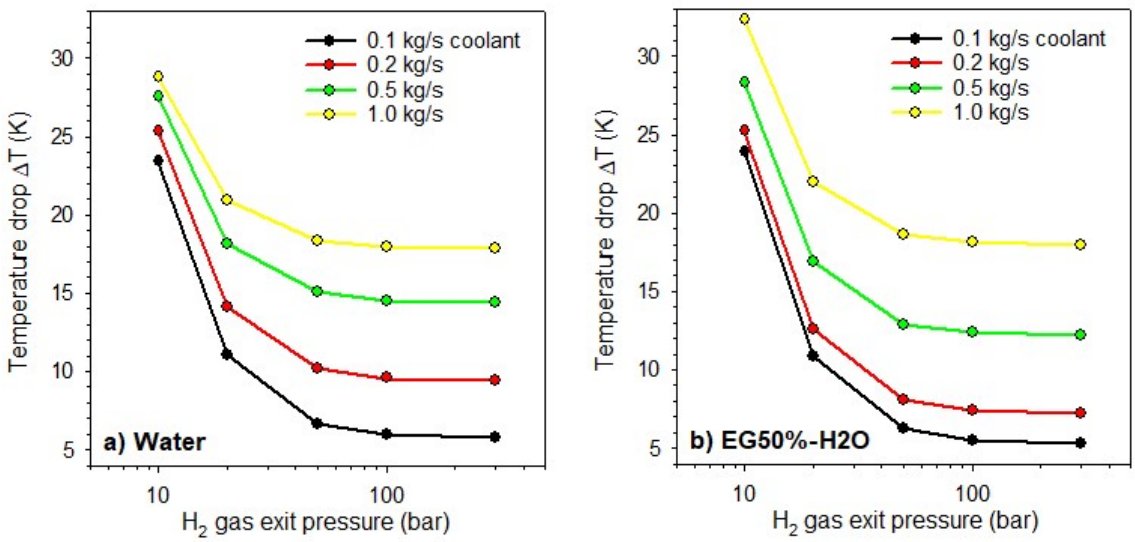

Figure 6: Variation of the temperature drop ΔT in the heat exchanger as function of gas exit pressure P_{out} for different coolant flow-rates using a) water at $T_c = 274$ K and b) EG50%-water at $T_c = 238$ K as coolants. The gas flow-rate was $\dot{m}_{H2} = 0.1$ kg/s with inlet temperature $T_{H2} = 298$ K.

3.4 Thermal behavour of coolants in heat exchangers

In order to understand why some coolants have higher cooling capacity and show better properties than others, one needs to look more into effects caused by their physical properties, in particular the heat capacity and viscosity. The values of these at the temperature of the coolant inlet are shown in Table 1. Typical values at the hydrogen gas inlet are also shown for comparison.

Figure 7 shows temperature distribution inside three different coolants i) pure water injected at 274 K (0.8°C), ii) EG30%-water injected at 259 K (−14°C), and iii) EG50%-water injected at 238 K (−35°C). Here, the plots are rotated and re-scaled for easier display. In the simulation the concentric tubes of the heat exchanger were horizontal with the H_2 injection from the left hand side, corresponding to the bottom of these plots. The coolant was entering

DocuSign Envelope ID: 2C0AE915-F5FC-4C21-ACD2-CF1A7BDE232A

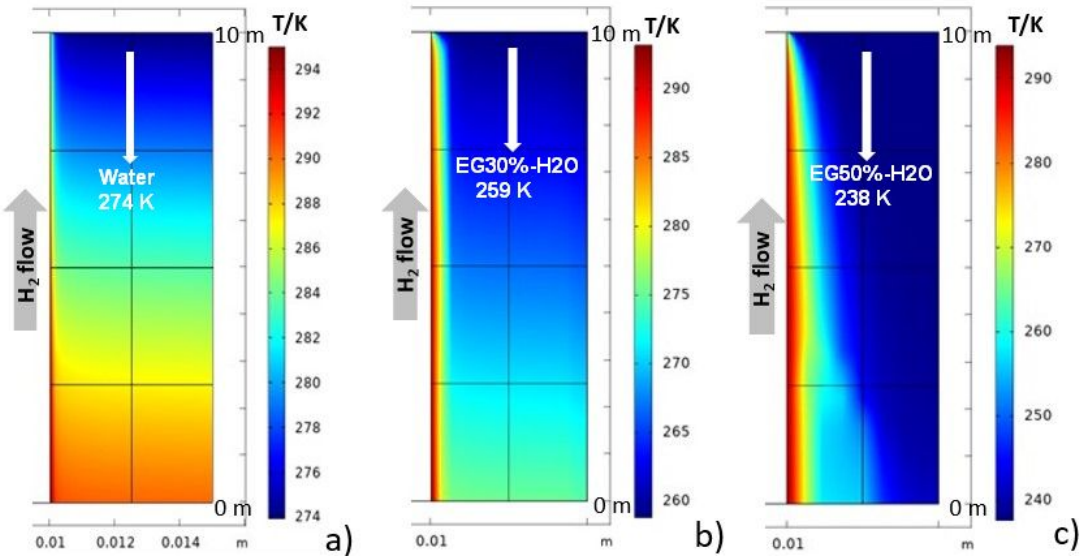

Figure 7: Temperatures in a cross section of the horizontal outer tube using a) water, b) 30% ethylene glycol-water mixture, and c) 50% EG-water mixture. The plots are rotated for clarity, and axis are out of scale. The width of the annulus for the coolant was 5 mm and the length was 10 m. Hydrogen gas was entering from the bottom left of each sub-figure and the coolants entering from the top of these images as indicated by arrows. The mass flow-rates of H_2 gas and coolants were the same in all cases, $\dot{m}_H = \dot{m}_c = 0.2$ kg/s with H_2 temperature T_{H2} =293 K.

Fluid	Temp. T	η / mPa·s	C_p / kJ/kg·K
H_2O	0°C	1.79	4.22
ethylene glycol (EG)	−17°C	75	2.23
EG30%-water	−14°C	7.9	3.61
EG50%-water	−35°C	60	3.00
H_2, 100 bar	20°C	0.009	14.5

Table 1: Values of the viscosity η and heat capacity C_p of water, ethylene glycol and some EG-water mixtures at the lowest temperature that they can be used (near freezing point). Values for hydrogen gas at pressure 100 bar is also shown for comparison.

from the right-hand side of the HX, corresponding to the top of these plots. As can be seen for water coolant Fig. 7a), the whole volume of coolant has been heated at the exit position of the tube (lower end of the plot). For the EG30%-water mixture in Fig. 7b), the temperature of most parts of the coolant near the exit was at 276 K, which corresponds to a coolant temperature increase of 17 K. Only a very thin fluid layer of thickness about 0.5 mm near the inner wall has been heated up to a temperature near that of the incoming warm gas (293 K). For the EG50%-water coolant (Fig. 7c)), the largest fraction of the liquid volume was not heated at all and was still at the inlet temperature of 238 K. This means that the capacity of this coolant has not been fully utilized, and a much longer heat exchanger will be needed to utilize the full cooling capacity of the liquid.

These effects can be seen more quantitatively in Fig. 8, which shows the radial temperature profile in the coolant tube for three different mass flow-rates for each of these coolants. The red coloured curves for coolant flow-rates $\dot{m}_c = 0.2$ kg/s corresponds to the cases shown in Fig. 7. For water there was a very even distribution of the absorbed heat throughout the entire bulk volume. For the mixture with 30% ethylene glycol (long dashed line), there is a small

DocuSign Envelope ID: 2C0AE915-F5FC-4C21-ACD2-CF1A7BDE232A

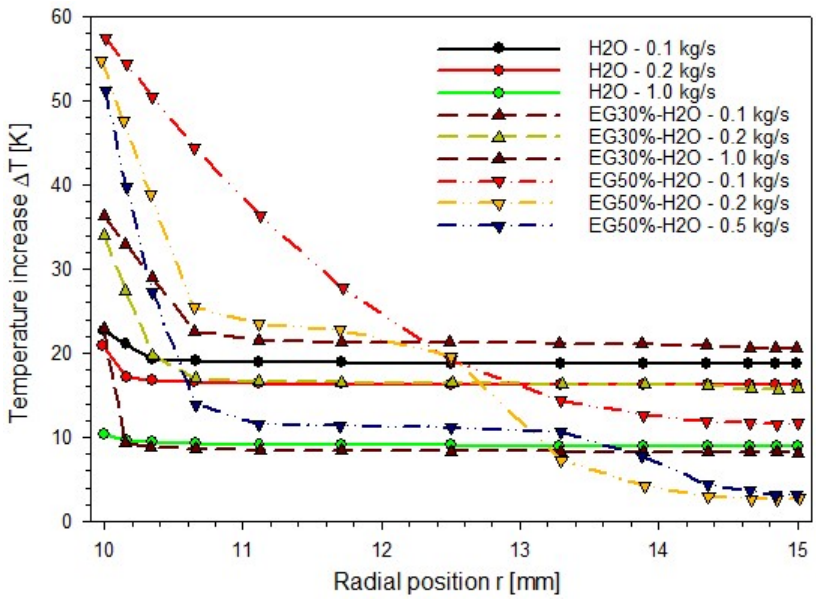

Figure 8: Temperature increase $T_{c,out} - T_{c,in}$ vs. radial position at coolant exit for various mass flow-rates $\dot{m}_c$. a) Pure water coolant, $T_c = 274$ K, b) 30% ethylene glycol-water mixture, $T_c = 259$ K, and c) 50% EG-water mixture, $T_c = 238$ K. The temperature and flow-rate of the hydrogen were the same in all cases, $T_{H2} = 293$ K and $\dot{m}_{H2} = 0.2$ kg/s.

increase of the temperature near the wall of the inner tube, while for the 50% EG mixture (dash-dot lines) this temperature gradient covers the whole fluid volume within the outer annulus. The temperature drop ΔT for H_2 in the inner tube averaged over the gas volume at the HX exit was 5.7 K, 5.1 K and 4.9 K for pure water, EG30% and EG50%, respectively. Thus, the temperature of the gas at exit was about 288 K (15°C) in all cases. However, the total cost of cooling in the three cases will be very different since cooling to −35°C or −14°C have a much larger energy cost than cooling water to 0°C − 1°C. In addition comes the cost of more expensive coolant fluids and higher costs of pumping caused by a larger pressure drop in the coolant tube.

The was no temperature gradient in the radial temperature profile at the exit of the inner hydrogen tube. Only in the case of the very cold EG50%-water mixture, some small temperature variations near the wall could be seen. This showed that the mixing within the gas was very good in all cases, mainly due to the turbulent character of the flow pattern.

3.5 Flow patterns in the heat exchanger

In order to understand why the very cold EG50%-water mixture behaves equal to, or even worse, than pure water when considering cooling capacity, one needs to look into the coolant flow patterns in the different cases. For the simulated dimension of the pipes and a mass flow-rate of 0.2 kg/s, the hydrogen gas velocity was $v_g = 83$ m/s and the velocity of the coolants was about $v_{cool} = 0.5$ m/s. The flow behavior of a fluid is determined by its Reynolds numbers $Re = \frac{\rho v \mathcal{L}}{\eta}$ where $\mathcal{L}$ is a typical length scale in the flow situation, i.e., diameter of a tube or separation between inner and outer wall in annular flow. Based on the properties and temperatures of the fluids at the entrance to the HX and flow-rates in the range $\dot{m} = 0.1 - 1$ kg/s, the range of values for Reynolds number were found to be $Re \approx (0.7-7)\cdot 10^6$, 730−7300, 162 − 1620, and 21 − 210 for H_2, water, EG30%-water, and EG50%-water, respectively. Since

DocuSign Envelope ID: 2C0AE915-F5FC-4C21-ACD2-CF1A7BDE232A

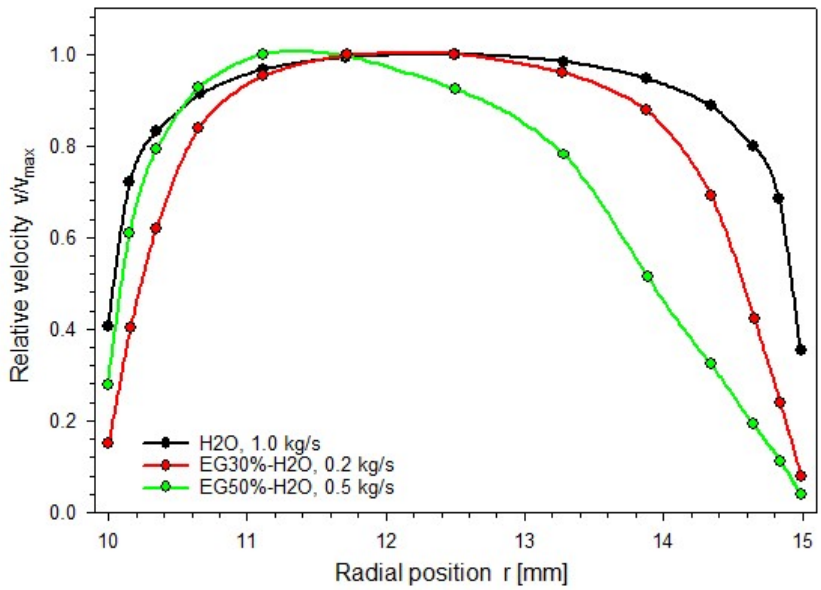

Figure 9: Calculated relative fluid velocity profiles at the coolant exit as function of radial position in the heat exchanger. The inner wall of the coolant annulus was at position $r = 10$ mm. The hydrogen gas flow-rate was $\dot{m}_{H2} = 0.2$ kg/s in all the three cases. The coolant mass flow-rates $\dot{m}_c$ and maximum velocities v_{cool} were $(\dot{m}_c, v_{cool}) = (1.0$ kg/s, 2.8 m/s), (0.2 kg/s, 0.60 m/s), and (0.5 kg/s, 1.7 m/s) for water, 30% ethylene glycol, and 50% EG water mixtures, respectively.

the value of Re for hydrogen was above the critical value for transition from laminar flow to turbulence in pipe flow, $Re_{crit} \sim 2300 - 3000$ [10], the gas flow was fully turbulent with very good mixing inside the fluid volume for all values of $\dot{m}_{H2}$. For water coolant flow at lower values of $\dot{m}_c$, the Reynolds number was below the reported value $Re_{crit} \sim 2500$ for transition for flow in an annulus with inner to outer radius ratio 2/3 [11], but the length of the heat exchangers still assured a complete thermal mixing at the exit position of the coolant tube. For water with higher values of $\dot{m}_c$, the flow was turbulent. However, for the ethylene glycol mixtures the flow was purely laminar independent of mass flow-rate, and the mixing of heat will be much slower.

Figure 9 shows the fluid velocity at the exit of the coolant annulus scaled with the maximum flow speed value in that case for three selected flow regimes, i) laminar, ii) near transition to turbulent, and iii) fully turbulent flow ($Re \approx 7300$). For water flow at speed $v_{cool} = 1.7$ m/s (case i)), the flow profile is not parabolic in shape as for flow in a tube but more flattened and still symmetric as in turbulent flows. For case iii), which is EG50%-water mixture with flow speed $v_{cool} = 1.7$ m/s, the profile is a skewed parabola with higher velocities near the warm inner wall. Here, near the wall, the fluid viscosity η has decreased relative to its value at the inlet due to the rise in temperature near the warmer wall. This results in a higher flow velocity than in the colder, outer parts of the fluid. The resulting shear flow will contribute to a slow mixing of the heat. The EG30%-water mixture (case ii) with flow speed $v_{cool} =$ 0.6 m/s showed some type of intermediate situation, both asymmetric shape and flattening at the top of the profile. The resulting temperature profiles for these examples were shown in Fig. 8. The full temperature map for the water case was similar to that shown for water at $\dot{m}_c = 0.2$ m/s in Fig. 7a), and the maximum cooling capacity has been utilized in this case. The EG30%-water case was the same as that shown in Fig. 7b). Here, a heat exchanger of

DocuSign Envelope ID: 2C0AE915-F5FC-4C21-ACD2-CF1A7BDE232A

longer length than the current $L = 10$ m would have utilized the coolant in a better way. For EG50%-water mixtures, higher flow velocities $\dot{m}_c$ will certainly increase the cooling power, but the utilization of the coolant and system efficiency may still be poor. Increasing flow-rate may help to increase shear mixing in the fluid flow.

4 Discussion

The temperature after filling can be calculated based on tables of heat transfer coefficients U for different flow-rates of gas and coolant, $\dot{m}_{H2}$ and $\dot{m}_c$, and the size of the heat exchanger (fluid contact area or length and tube radii). In addition, the initial temperatures and pressures of the large storage tank and the smaller vehicle fuel tank are input parameters. The pressure in the fuel tank when filled to maximum hydrogen mass content (in kg) will often be higher than the nominal pressure in the tank (350 or 700 bar) but will drop down to the operating pressure as the gas cools down to the ambient temperature via the tank walls. Reaching about $20 - 25$°C, the pressure will drop to the normal operation pressure. If this stop-filling pressure is too high relative to the maximum pressure limit, the tank has to be filled to less than its maximum capacity.

Examples of filling two commercially available tanks of different sizes are shown in Fig. 10, which shows the temperature at end of filling using different coolant flow-rates for water and EG-water mixtures. The average temperature inside the tank was calculated using the Engineering Equation Solver (EES) software [12] with values of the heat exchange coefficient U for the coolants calculated using COMSOL, as described above. Typical values of U for various gas and coolant flow-rates are listed in the tables in Appendix 2. As can be seen from these tables, the heat exchange is more efficient from water than from the water mixtures. However, the lower coolant temperature that can be used in the mixtures, can lead to a lower final temperature in the gas.

Figure 10a) shows that for smaller tanks with capacity of 10 kg H_2 and gas flow-rate of 3 kg/min (i.e., filling time about 3 min 20 s) all coolants with flow-rate above 1 kg/min will manage to keep the tank temperature well below $T_{max} = 85$ °C. However, this maximum temperature may depend on the tank vendor, and with a lower temperature limit, like $T_{max} = 65$ °C, EG-water coolants with flow-rates $\dot{m}_c \geq 30$ kg/min may be needed. For a larger sized tanks, like one with capacity 46 kg of H_2 in Fig. 10b), coolant flow-rates of at least 10 kg/min will be needed during filling to keep the tank temperature below 85 °C. It may be noted that for a hydrogen mass flow-rate of 3 kg/s, it is only at the highest coolant flow-rates $\dot{m}_c >$ 20 kg/min that clear differences in capacity among the three coolants can be seen. For the EG-water mixtures, the heat will only be absorbed by a thin layer of fluid close to the wall of the inner tube, and the utilization of the total cooling capacity of these mixtures are low. By recycling the coolant mixtures after the HX exit using an external stirrer, the coolant may be re-used since the bulk temperature increase of the coolant after mixing will be relatively small. Alternatively, the coolant mixtures will be recycled via an external cooler. Future studies will focus on how optimizing the HX tube dimensions can affect the heat exchange and the final fuel tank temperature.

Based on the initial state of the hydrogen gas in the large storage tank, the final state of the gas in the fuel tank, and the mass flow-rate $\dot{m}_{H2}$, one can estimate the cooling capacity

DocuSign Envelope ID: 2C0AE915-F5FC-4C21-ACD2-CF1A7BDE232A

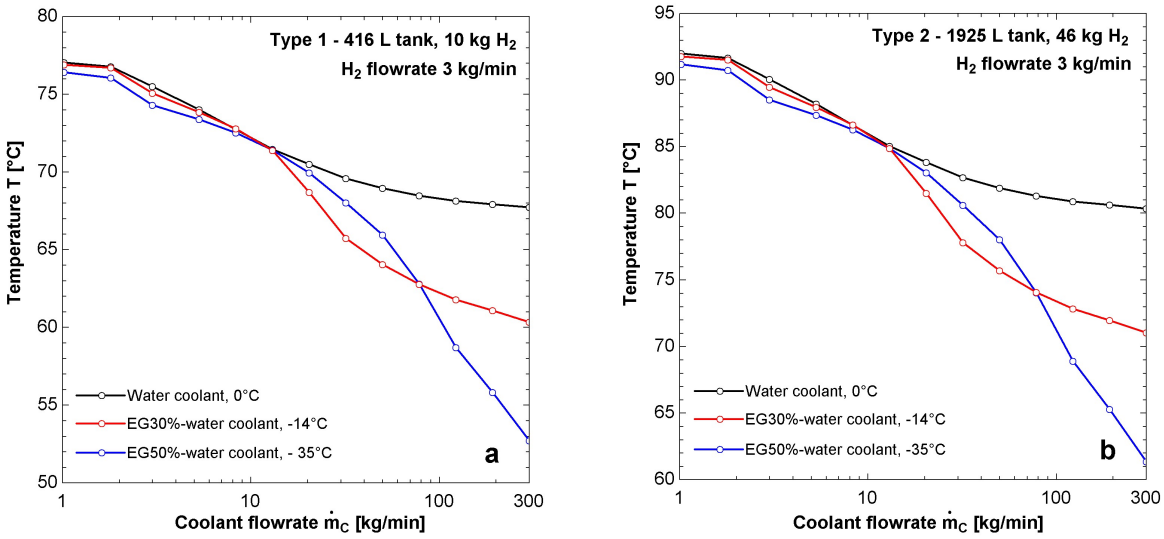

Figure 10: Temperature inside H_2 tanks at end of filling as function of coolant mass flow-rate $\dot{m}_c$ using three different coolants. Tanks of two different sizes, a) vol= 416 L, and b) vol= 1925 L are compared. In the calculation, they were filled from 20 bar pressure up to max storage capacity at 350 bar and ambient temperature, 10 kg and 46 kg of H_2, respectively. The initial temperature of H_2 gas and the tanks were 20°C, and the heat capacities per unit area of the tank surfaces were assumed to be the same.

(in kW) available from the coolants discussed above. This analysis is presented in Appendix 3.

This report has discussed heat transfer using some selected coolants in a simple double pipe heat exchangers. There exists a large literature on how passive or active modifications of such devices can improve heat transfer, including tube inserts, wall modifications and stirrers to get better flow mixing. This is summarized in a review article from 2017 by M. Omidi, M. Farhadi, and M. Jafari [13]. Some studies published after that are given in Refs. [14]−[21]. Use of nanoparticles added to the coolant in order to increase the thermal coupling has also been studied, and this has been summarized by Hajatzadeh et al. [22] and by Louis et al. [23]. All these types of modifications can increase the heat transfer rate by a considerable amount but will also increase the pressure drop across the tubing and thereby the pumping power needed. Thus, there is an energy cost for all such improvements. Finally, a compressed hydrogen storage system for fast filling of hydrogen gas has been studied by Li et al. [24] and Bourgeois et al. [25]. Kesana et al. [26] have recently published a study on simulating temperature distributions within small and large gas storage tanks during filling.

Acknowledgement

This work was supported in part by the Research Council of Norway KPN project no. 294568 “H2 Maritime” and by WP9 under the EU HORIZON-ER-JU-2022-01 FP4 project no. 101101917 “Rail4EARTH”, a part of the “Europe’s Rail” program.

DocuSign Envelope ID: 2C0AE915-F5FC-4C21-ACD2-CF1A7BDE232A

References

[1] https://projects.rail-research.europa.eu/eurail-fp4/

[2] J.H. Lienhard IV and J.H. Lienhard V, *A Heat Transfer Textbook* (Phlogiston Press, Cambridge, MA, 2020), https://ahtt.mit.edu/

[3] D. Taler, *Numerical Modelling and Experimental Testing of Heat Exchangers*, (Springer, 2019) ISBN 978-3-319-91128-1

[4] O. Levenspiel, *Engineering Flow and Heat Exchange*, (Springer, 2014) ISBN 978-1-4899-7454-9

[5] G. Nellis and S. Klein, *Heat transfer*, (Cambridge University Press, 2009) ISBN 978-1-107-67137-9

[6] https://www.linquip.com/blog/efficiency-of-heat-exchanger/

[7] Comsol Multiphysics - https://www.comsol.com/

[8] G. Helgesen, *Heat exchangers for hydrogen tank filling*, IFE-report no. IFE/E-2023/002, ISBN: 978-82-7017-940-4 (2023)

[9] SAE J 2601-2-2014 protocol, *Fueling Protocol for Gaseous Hydrogen Powered Heavy Duty Vehicles*, https://www.sae.org/standards/content/j2601/2_201409/

[10] S. Rodrigues, *Applied Computational Fluid Dynamics and Turbulence Modeling* (Springer, 2019), ISBN 978-3-030-28691-0, doi.org/10.1007/978-3-030-28691-0

[11] H. Dou, B. Khoo, and H. Tsai, *Determining the critical condition for turbulent transition in a full-developed annulus flow,* J. Petroleum Science and Engineering, **73**, 41 (2010)

[12] Engineering Equation Solver - https://fchartsoftware.com/

[13] M. Omidi, M. Farhadi, and M. Jafari, *A comprehensive review on double pipe heat exchangers,* Applied Thermal Engineering, **110**, 1075 (2017)

[14] M. Hashemian et al., *Enhancement of heat transfer rate with structural modification of double pipe heat exchanger by changing cylindrical form of tubes into conical form,* Applied Thermal Engineering, **118**, 408 (2017)

[15] R. Hosseinnezhad et al., *Numerical study of turbulent nanofluid heat transfer in a tubular heat exchanger with twin twisted-tape inserts,* Journal of Thermal Analysis and Calorimetry, **132**, 741 (2018)

[16] A. Peccini et al.*, Optimal design of double pipe heat exchanger structures,* Industrial and Engineering Chemistry Research, **58**, 12080 (2019)

[17] M Ali and R. Jalal, *Experimental investigation of heat transfer enhancement in a double pipe heat exchanger with a twisted inner pipe,* Heat Transfer, **50**, 8121 (2021)

DocuSign Envelope ID: 2C0AE915-F5FC-4C21-ACD2-CF1A7BDE232A

[18] T. Dagdevir and V. Ozceyhan, *An experimental study on heat transfer enhancement and flow characteristics of a tube with plain, perforated and dimpled twisted tape inserts,* International Journal of Thermal Sciences, **159**, 106564 (2021)

[19] L. Wang, Y. Lei and S. Jing, *Performance of a Double-Tube Heat Exchanger with Staggered Helical Fins,* Chemical Engineering and Technology, **45**, 953 (2022)

[20] Q. Hu et al., *Experimental and numerical investigation of turbulent heat transfer enhancement of an intermediate heat exchanger using corrugated tubes*, International Journal of Heat and Mass Transfer, **185**, 122385 (2022)

[21] S. Marzouk et al., *A comparative numerical study of shell and multi-tube heat exchanger performance with different baffles configurations,* International Journal of Thermal Sciences, **179**, 107655 (2022)

[22] A. Hajatzadeh et al., *An updated review on application of nanofluids in heat exchangers for saving energy,* Energy Conversion and Management, **198**, 111886 (2019)

[23] S. Louis et al., *Application of Nanofluids in Improving the Performance of Double-Pipe Heat Exchangers—A Critical Review,* Materials, **15**, 6879 (2022)

[24] J. Li et al., *An analysis on the compressed hydrogen storage system for the fast-filling process of hydrogen gas at the pressure of 82 MPa*, Energies, **14**, 2635 (2021)

[25] T. Bourgeois et al.,*The temperature evolution in compressed gas filling processes: A review*, Internat. J. Hydrogen Energy, **43**, 2268 (2018)

[26] N. Kesana et al., *Modelling of fast fueling of pressurized hydrogen tanks for maritime applications,* Internat. J. Hydrogen Energy **48**, 30804 (2023)

DocuSign Envelope ID: 2C0AE915-F5FC-4C21-ACD2-CF1A7BDE232A

A Appendix 1: Dimensionless numbers in heat exchangers

Sometimes it may be convenient to calculate the parameters of a heat exchangers using dimensionless numbers. This can be done by introducing the dimensionless number called *Number of Transfer Units NUT* defined as

$$NTU = \frac{UA_s}{(\dot{m}c_p)_{min}}, \tag{8}$$

where subscript *min* refers to the smallest of the values of the heat flow capacities, $\dot{C} = \dot{m}c_p$, for the hot and the cold fluids. Here, U is the effective heat transfer coefficient (unit W/m^{2}K), A_s is the contact area between fluids in the heat exchanger, $\dot{m}$ is the fluid mass flow-rate, and c_p is the specific heat capacity of the fluid. Also, it is common to define the *capacity ratio* C_r as

$$C_r = \frac{(\dot{m}c_p)_{min}}{(\dot{m}c_p)_{max}}. \tag{9}$$

The *effectiveness* of the heat exchanger can then be written as a function of NTU and C_r, $\varepsilon = \varepsilon(NTU, C_r)$. For counter-flow HX, the relationship between NTU and ε is

$$\varepsilon = \frac{1 - \exp\left[NTU(C_r - 1)\right]}{1 - C_r \cdot \exp\left[NTU(C_r - 1)\right]}. \tag{10}$$

Effectiveness ε as a function of NTU and C_r for various types of heat exchangers can be found in tables. The ε-value increases strongly with NTU for $NTU < 1.5$ and then levels off as can be seen in Fig. 11, which is for a counter-flow heat exchanger. For fixed value of NTU, ε increases with decreasing C_r, most clearly for $NTU > 2$. However, this C_r-dependence is smallest for counter-flow heat exchangers.

Referring to Fig. 6a) in the main text, for the water coolant at P_{out} =100 bar and $\dot{m}_c$ = 0.2 kg/s, the values are $NTU = 1.43$ and $\varepsilon = 0.66$, while at $\dot{m}_c = 1.0$ kg/s the values are $(NTU, \varepsilon) = (1.59,\ 0.74)$. However, using EG50%-water and $\dot{m}_c = 1.0$ kg/s as in Fig. 6b), the effectiveness is only $\varepsilon = 0.30$ for an NTU-value of 0.39. Thus, the heat exchange can be much improved.

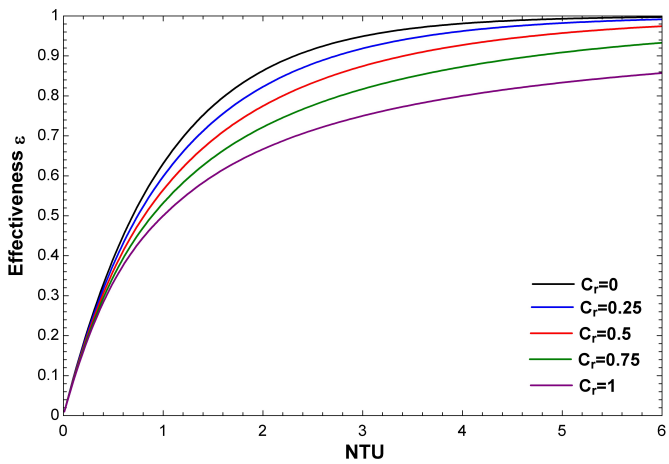

Figure 11: Effectiveness ε as function of NTU and C_r for counter-flow heat exchanger. The colours are for different values of capacity ratio C_r.

DocuSign Envelope ID: 2C0AE915-F5FC-4C21-ACD2-CF1A7BDE232A

B Appendix 2: Heat transfer coefficients

Values of the effective heat transfer coefficient calculated as described in the main text for a concentric pipe counter-flow heat exchanger of length $L = 10$ m with inner tube radius r_i= 10 mm and outer tube radius r_o= 15 mm.

Coolant mass flowrate $\dot{m}_C$ [kg/s]	Gas mass flowrate $\dot{m}_{H2}$ [kg/s]							
	0.005	0.01	0.02	0.05	0.1	0.2	0.3	0.5
0.02	260.9	325.7	383.6	435.1	452.9	452.1	438.6	410.9
0.05	331.7	417.5	506.7	623.8	689.3	724.2	724.7	700.5
0.1	459.7	643.4	855.9	1137	1307	1415	1440	1428
0.2	542	799	1116	1586	1915	2163	2253	2304
0.5	608.5	945	1411	2169	2781	3339	3606	3852
1	655.9	1049	1630	2704	3679	4667	5195	5766
2	928.2	1170	1839	3212	4620	6199	7117	8232
5	615.3	1301	3050	4004	5878	8296	9900	12043

Table 2: Heat transfer coefficients U in W/(m^{2}K) for various H_2 gas mass flow-rates $\dot{m}_{H2}$ using **water as coolant** with mass flow-rates $\dot{m}_c$.

Coolant mass flowrate $\dot{m}_C$ [kg/s]	Gas mass flowrate $\dot{m}_{H2}$ [kg/s]							
	0.005	0.01	0.02	0.05	0.1	0.2	0.3	0.5
0.02	183.7	204.2	217.9	229.9	235	236.4	234.8	229.6
0.05	204.5	238.7	267.7	300.9	318.3	327.5	328.4	323.5
0.1	248.5	311.3	372.4	428.5	453.3	467.2	471.1	471.9
0.2	303.8	372.1	441.4	565.7	674.8	766	799.1	805.7
0.5	510.6	737.9	1013	1404	1688	1927	2034	2125
1	597.2	894.7	1301	1938	2425	2844	3041	3232
2	727.8	1019	1518	2386	3115	3809	4168	4548
5	627.9	1453	2084	3192	4414	5748	6510	7409

Table 3: Heat transfer coefficients U in W/(m^{2}K) for various H_2 gas mass flow-rates $\dot{m}_{H2}$ using a **30% ethylene glycol - water mixture as coolant** with mass flow-rates $\dot{m}_c$.

Coolant mass flowrate $\dot{m}_C$ [kg/s]	Gas mass flowrate $\dot{m}_{H2}$ [kg/s]							
	0.005	0.01	0.02	0.05	0.1	0.2	0.3	0.5
0.02	163.3	180.5	191.2	199	201.9	203	202.3	199.6
0.05	178.7	199.1	212.6	222.7	226.7	228.7	229.2	229
0.1	198.7	222.4	238.7	251.7	257.5	262	263.2	262.6
0.2	226.4	260	285.8	314.9	333.8	346.9	350.5	349.3
0.5	276.3	335.5	393.6	490.9	587.3	661.5	692.8	698.7
1	331.6	422.9	517.9	695.3	901.6	1070	1176	1292
2	398.8	551	787.4	1212	1528	1780	1890	1989
5	578.4	1478	1537	2109	2603	3062	3294	3536

Table 4: Heat transfer coefficients U in W/(m^{2}K) for various H_2 gas mass flow-rates $\dot{m}_{H2}$ using a **50% ethylene glycol - water mixture as coolant** with mass flow-rates $\dot{m}_c$.

The inlet temperature of the hydrogen gas in the simulations was $T_{H2} = 27$°C and that of the coolants $T_c = 0$°C, -14°C, and -35°C for water, EG30%-water, and EG50%-water, respectively. The exit pressure of the gas from the HX was 100 bar.

DocuSign Envelope ID: 2C0AE915-F5FC-4C21-ACD2-CF1A7BDE232A

C Appendix 3: Cooling capacity

In order to estimate the cooling capacity needed to cool the incoming hydrogen gas to a certain temperature at the inlet of the gas fuel tank, some calculations were done for a few selected cases. In this example, a composite material type 4 tank of intermediate size with volume 2 m^2 and diameter 70 cm was chosen. Further, it was assumed that both the large storage tank and the fuel tank were at initial temperature of $T_{init} = 15°C$, the pressure in the storage tank was 450 bar and the fuel tank was empty ($P \approx 1$ bar). A fuel tank of this size can store 48 kg of H_2 at p =350 bar and $T = 15°C$. However, just after the filling to max capacity 48 kg has been completed, both the temperature T_{final} and pressure P_{final} in the tank will be much larger than ambient temperature and planned filling pressure. After some time, which will depend on the heat conductivity of tank walls and ambient conditions in the surrounding air space, both T and P will drop down to the nominal values for a tank containing 48 kg of H_2. An estimate for the heat capacity of the tank walls was used in these calculations since some of the heat generated during gas expansion will be taken up by the walls. Any cooling from the external side of the tank walls has not been included in this calculation since that will depend a lot on the heat convection in the air surrounding the tank.

Three cases were studied:

i) Gas cooled from $T_{init} = 15°C$ to inlet temperature $T_{in} = 0°C$ before entering the fuel tank (e.g., by cold water)

ii) Gas cooled to $T_{in} = -14°C$ before entering (e.g., by efficient cooling by an EG30%-water mixture)

iii) Gas cooled to $T_{in} = -40°C$ before entering (e.g., by efficient cooling by an EG60%-water mixture)

The cooling power for pre-cooling during filling for different gas flow-rates, as well as the time needed to fill the tank to maximum capacity of 48 kg of hydrogen, have been calculated in each of the cases. The change in enthalpy H mainly depends on the temperature drop $\Delta T = T_{init} - T_{in}$ during cooling. The enthalpy change per kg, as well as the total value $\Delta H_{48\,kg}$ for the 48 kg of gas, are listed in the fourth and fifth column of Table 5.

The needed cooling capacity will only depend on how fast the filling will occur. The results for cooling power vs. H_2 flow-rate for the three cases are shown as solid lines in Fig. 12. Also, the required filling time for a certain flow-rate is shown as a dashed curve in this figure. The solid lines are labeled with gas inlet temperature (T_{in}), final temperature (T_{final}), and final pressure (P_{final}) in the tank at complete filling. These values are also summarized in the table below. The sixth column of this table gives the the slopes of the coloured lines, $\frac{\mathrm{d}Power}{\mathrm{d}(\dot{m}_{H2})}$, which can be used for finding the exact kW-value in each case. As can be seen from this figure, lower

T_{in} [°C]	T_{final} [°C]	P_{final} [bar]	$H_{15°C} - H_{T_{in}}$[kJ/kg]	$\Delta H_{48\,kg}$ [kWh]	$\frac{\mathrm{d}Power}{\mathrm{d}(\dot{m}_{H2})}$[kW/(kg/min)]
0	84	437	223	2.97	3.68
-14	73	423	431	5.74	7.16
-40	52	398	816	10.88	13.61

Table 5: Parameters related to the filling processes shown in Fig. 12: i) Inlet temperature T_{in}, ii) final tank temperature T_{final}, iii) final tank pressure P_{final}, iv) enthalpy change per kg of H_2, v) total enthalpy change on cooling 48 kg of gas from 15°C to T_{in} before fuel tank inlet, and vi) slope of power vs. flow-rate lines in the figure.

DocuSign Envelope ID: 2C0AE915-F5FC-4C21-ACD2-CF1A7BDE232A

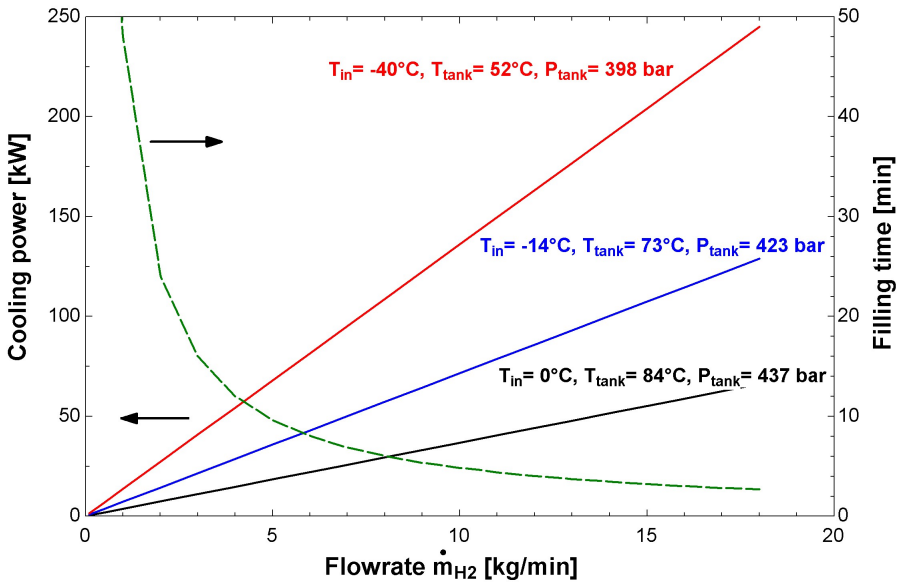

Figure 12: Cooling power needed for the heat exchanger in the cases i) black line, ii) blue line, and iii) red line described in the text above. The filling time needed for each value of $\dot{m}_{H2}$ is the same for all cases and is shown by the green dashed curve.

mass flow-rates of gas, and correspondingly longer filling time (green dashed curve), lead to smaller needs of cooling capacity.

In the current simplified model, the final temperature and pressure in each case will be independent of the gas flow-rate. However, in a realistic real case the heat transported through the tank wall during the longer filling time at small flow-rates will lead to lower temperatures at end of filling than those shown in this table. In all cases, the final temperatures were below the temperature limit of $T_{max} = 85°\text{C}$ for type 4 composite tanks. The final pressures are well above the nominal tank pressure of 350 bar. A consequence of this is that one cannot fill the tank to its maximum mass capacity unless the maximum allowed pressure in the tank is well above 400 bar.

As an example, the needed cooling power is 21.5 kW for $\dot{m}_{H2} = 3$ kg/min when the gas inlet temperature is $T_{in} = -14°\text{C}$ (blue line in Fig. 12). Cooling the gas from ambient temperature 15°C to this low temperature requires a high mass flow-rate of the coolant. Based on the heat exchanger model presented in the main text and using a EG30%-water mixture at flow-rate $\dot{m}_c = 5$ kg/s = 300 kg/min (Table 3), it was found that maximum cooling power was about 20 kW, slightly below what is needed. However, using EG50%-water mixture at $-35°\text{C}$ with $\dot{m}_c = 2$ kg/s = 120 kg/min, a cooling power value of 23 kW, $T_{in} = -16°\text{C}$, and $T_{final} = 71.4°\text{C}$ can be obtained.

For larger values of gas flow-rate, $\dot{m}_{H2} \gg 3$ kg/min, both cooling power and coolant mass flow-rate will increase significantly and may go beyond the capability for cooling power of counter-flow heat exchangers as discussed in this report.